Hindawi
Advances in Materials Science and Engineering
Volume 2022, Article ID 1612539, 11 pages
https://doi.org/10.1155/2022/1612539

Research Article

Optimizing WEDM Parameters on Nano-SiC-Gr Reinforced Aluminum Composites Using RSM

R. Saravanan,[1] **G. Anbuchezhiyan**,[1] **Vamsi Krishna Mamidi**,[2] **and Palani Kumaran**[3]

[1]*Institute of Mechanical Engineering, Saveetha School of Engineering, Saveetha Institute of Medical and Technical Sciences (SIMATS), Chennai 602105, Tamil Nadu, India*
[2]*Department of Mechanical Engineering, Sri Venkateswara College of Engineering, Tirupati 517507, Andhra Pradesh, India*
[3]*Department of Mechanical Engineering, College of Engineering, Wolaita Sodo University, Wolaita Sodo, Ethiopia*

Correspondence should be addressed to R. Saravanan; dr.sarravanan@gmail.com, G. Anbuchezhiyan; tsgaaa1981@gmail.com, and Palani Kumaran; pkumaran2003et@gmail.com

Received 4 January 2022; Revised 2 March 2022; Accepted 20 April 2022; Published 28 May 2022

Academic Editor: Chang Chuan Lee

Nanocomposites are preferred for performance enhancement over micron composites because of their better performance in enhancing the desired properties of the parent material. Nano-silicon carbide and nano-graphite are considered together for reinforcement of Al7075 in this piece of research. Here, the purpose of reinforcement of graphite considered is to improve machinability. The stir casting was employed for fabrication of nanocomposite. The composite matrix includes Al7075 matrix material, reinforcement material of nano-SiC (5 wt.%), and nano-graphite (5 wt.%). Wire cut Electrical Discharge Machining (WEDM) of the synthesized nanocomposite SiC/Gr/Al7075 is considered for investigating the machinability. The objectives of the study are to synthesize the novel nanocomposite and optimize the process parameters to minimize the kerf width during WEDM. The independent variables like choice of wire electrode including the uncoated brass wire, diffused annealed wire, and zinc coated brass wire were considered along with operating parameters like gap voltage, pulse-off time (T_{off}), and pulse-on time (T_{on}). The response surface methodology (RSM) is used for designing experiments and analyzing and optimizing independent parameters of WEDM for minimizing the kerf width. Experimental results reveal that the machinability performance of the novel nanocomposite in WEDM with zinc coated brass wire was the best and produced minimum kerf width with the optimized inputs of 117 μs pulse-on time, 60 μs pulse-off time, 160A input current, and 10 volt gap voltage.

1. Introduction

As the aluminum of grade Al7075 is lightweight compared to its strength, it has vast application in aviation, automobiles, aerospace, marine, etc. [1] as well as meeting the material requirements globally [2]. Therefore, alteration of such material properties through composite technology and utilizing the excellence of nano-silica are the objectives of this research. The reinforcement selection is based on the properties to be altered. For example, if aluminium is reinforced with silica, it will enhance the hardness. If graphite included in aluminium matrix as a reinforcement agent, it will improve machinability as it possesses self-lubricating nature. Various ashes are derived from organic agricultural waste such as bagasse, coconut, and fly ash included in the aluminium matrix which will improve the yield strength and tensile strength [3]. The Al6061 with 4 wt.% graphite reinforcement offered 191.65 MPa of ultimate tensile strength and showed the trend of increase of reinforcement percentage increases the UTS. Aluminum with 6 wt.% offered 121.40 MPa of UTS with the trend of increase of reinforcement percentage increases the UTS. References [4, 5] altered tribological properties of AA7075 aluminium alloy like friction and wear properties by hybrid reinforcement of SiC and B4C. Reference [6] altered the composition of Al7075 for optimizing the wear behavior by reinforcing the alumina particles. Reference [7] utilized the SiO2 reinforcement for improving mechanical properties of

Al6061 and reported that the minimal particle size (170 μm) offered superior property enhancement compared to the particle size of 850 μm. Hence, this investigation utilized nano-SiC reinforced Al7075 with reduced concentration to enhance the mechanical properties.

The traditional machining may not fit due to the issues of serious tool wear due to reinforcement material properties, and hence tool life will be shortened [8, 9]. The electrical material or material reinforcement is found comfortable in machining EWEDM [10]. WEDM is generally preferred as it is cost effective in machining complex shapes as well as hard material machining as inferred in Figure 1 [11, 12]. TiN/Si3N4 nanocomposite machinability was investigated in WEDM, and it was found that higher pulse-off time offered low MRR [13]. With the collection of several small sparks between the gap of wire and job, the job that gets eroded is the principle behind the WEDM. Based on this phenomena, machining hard materials is taken place [14–16] adapted WEDM for machining the MMC of ZC63/SiCp as conventional machining methods incurred serious tool wear. The use of zinc coated wires helps to achieve the delivery of high useable energy at machining zone, maintain the stable discharge while cutting, and improve the rate of machining. Hermanni and Fleisbach also proved in their experiments and reported that brass coated with zinc performance is more appreciable than the use of copper wires by diffusion annealing [15]. This investigation is unique, and it compares the outcome of the input factors, as well as their impact on the kerf gap, statistically by ANOVA as suggested in [16]. The response surface methodology-based design of experiments was utilized to optimize the independent parameters like gap voltage and pulse times, like pulse-off and pulse-on, as well as discharge current for minimizing the dependent variable of kerf width. Reference [17] preferred WEDM to investigate the machinability of strength armor steel and optimized the MRR and SR, similarly for machining SKD11 steel [18], aluminum oxide-based ceramic [19], Nimonic C-263 superalloy [20], polycrystalline silicon [21], and HSLA steel [22] used in the WEDM for machinability investigation. As the hardness and toughness properties were enhanced in the Al7075 in this investigation also preferred machining the synthesized nanocomposite by WEDM. Aluminum and its alloy modification to alter the properties are reported widely in the literature. Some of the notable findings are discussed here. SiC reinforced aluminum metal matrix was investigated in terms of machinability at WEDM. Four process parameters were considered, namely, pulse-on, pulse-off, wire feed rate, and current, among which the pulse-on time was the most influencing factor [23]. Al/SiCp20 developed and investigated its machinability in WEDM process. [24] developed a hybrid composite by means of nonmetallic reinforcement in the aluminium matrix, and such composite's machineability performance was investigated in WEDM. They concluded that the surface roughness on machined surface increased with increase of quantity of machining parameters as well as increase of reinforcement quantity in the composite [25]. Machinability of a hard material, namely, Altemp HX, was investigated for WEDM process, and RSM was employed for optimizing the process parameters and developed a prediction model with a combination of an artificial neural network and genetic algorithm [26]. Nanocomposite is notable area of research; by using this technology, the wearability of marking paint was improved [27] nanocomposites not only limited to metal matrix but also applicable for polymer composites it is evident that Lead sulfide nanoparticles were utilized to develop the MDMO-PPV polymer film for optical applications [28] and the functionally graded carbon nanotube-reinforced composite developed for a biomedical application by [29]. Reference [30] developed nanocomposite coating for preventing blistering or delaminating and for corrosion protection [31]. Nanocomposite microelectrode were developed for the use of cerium oxide nanoparticles for cholesterol sensing application [31]. Some special types of nanocomposites like Fe3O4/graphene oxide/chitosan are for biomedical applications [32]. Hydroxyapatite-multiwalled carbon nanotube (HAp-MWCNT) coatings were developed to coat Ti6Al4V for biomedical application [33]. Multiwalled carbon nanotubes were also utilized to develop nanocomposite flexible films [34]; hence, the nanocomposite exhibited its promising improvement compared to micro-level reinforcement; hence, this study aims to develop a novel nanocomposite, namely, SiC/Gr/Al7075, and investigates its machinability in the WEDM process.

The novelty of this study includes the machinability performance of the synthesized novel nanocomposite SiC/Gr/Al7075 in WEDM process. Usually, new material is characterized in terms of physical, chemical, and mechanical as well as machinability aspects. This manuscript aims to investigate the machinability of the synthesized composite samples. The kerf width is a measurement of the total of wire diameter and gaps in workpiece. If it is wider, the accuracy of cut will be minimized and it restricts machining some sharp or complex profile in the work. Hence, the minimum kerf width is desirable. Therefore, the objective of the study is to optimize the process parameters and wire electrode for minimizing the kerf width in the WEDM of newly synthesized nanocomposite samples.

2. Materials and Methods

The chemical composition of prepared SiC/Gr/Al7075 nanocomposite is presented in Table 1, which is outcome of chemical characterization of a sample which was reinforced with 5 wt.% nano-SiC as well as 5 wt.% Gr. In this investigation, the SiC/Gr/Al7075 nanocomposite was produced by standard stir casting process. This composite is focused to develop material for automobile as well as aviation endeavors. Nano-SiC and nano-Gr of average size of less than 5 nanometers were utilized for reinforcement. The stirring speed was altered during reinforcement, and care was taken to prevent the loss of reinforcement. Figure 2 shows the photograph of preparation of novel nanocomposites.

The novel nanocomposite was synthesized in the stir casting setup of bottom poring type which includes mechanical stirrer, a furnace, and a reinforcement feeder. The stir prevents the sedimentation of solid particles that settle at bottom and helps to mix thoroughly the reinforcement

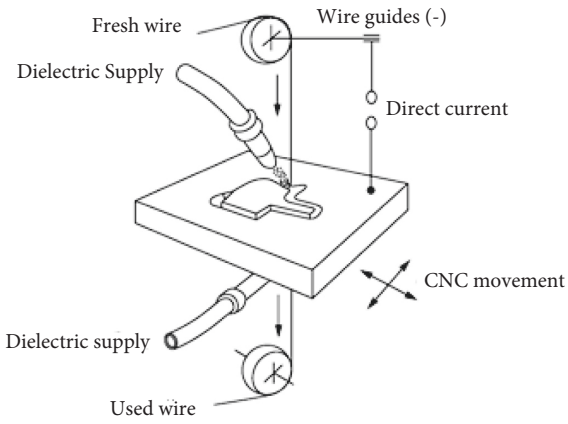

Figure 1: Schematic illustration of WEDM setup [14].

materials. The sequence of preparing the sample is as follows: Initially, Al7075 material was charged (90%) in the furnace and melted. The molten metal was stirred with help of mechanical stirrer, the reinforcement materials nano-SiC (5 wt.%) and nano-graphite (5 wt.%) were fed through feeder and stirred continuously, and the molten temperature was maintained between 700°C and 750°C at the time of pouring. The stirring speed was maintained at 700 rpm. The composite molten metal was poured in the mould and allowed to solidify. The sample was finished with grinding and prepared for machining investigation.

The proposed nanocomposite is developed for machining the components which featured with intricate shape and which are difficult to produce in conventional machining. So, the machineability of proposed composite is preferred to test in WEDM process.

2.1. Selection of Wire Electrodes. Zinc coating is generally preferred considering its unique advantages in EDM process; for example, it has a lesser vaporization point as well as lesser melting point as compared to alternate wire material of copper, it improves rate of machining, and the volume of zinc in the wire is limited to 40% as it loses the properties requirements for WEDM process. Hence, the 60/40 Cu/Zn ratio is generally chosen for higher cutting speed requirements, with layer thickness limited to 2-3 μm on either copper or brass wires for WEDM process [15]. Another way to coat the wire is to immerse it in hot water. It is a less precise and faster process of coating, and the wires are usually less expensive. In this investigation CuPbZn/Zn coated wire is preferred. Though EDM electrodes with 40% zinc content are preferable, they are difficult to produce due to some manufacturing limitations. This necessitates the development of a new process for producing wire with a higher zinc surface. Copper or brass wires could be coated with pure zinc in the rage of 18 μm to 35 μm. The pure zinc coating diffuses during annealing in a specific furnace so the mixture prepared for targeting values 45% to 47% and by considering diffusion 50% zinc and 50% brass is used. Hence, higher zinc content was achieved compared to direct manufacturing method. These wires are termed as diffusion-annealed wires. They are control group and are widely employed in WEDM for machining various hard metals and complicated profiles, created by combining zinc and copper. Brass wires for EDM are commonly an alloy with a Cu/Zn ratio ranging from 63/37 (American and European) to 65/35 (Australian and New Zealand) (Asian). In the present experimentation, we used 0.25 mm diameter uncoated brass wire and diffused and zinc coated brass wires (electrode).

Table 1: Chemical constituents of SiC/Gr/Al7075 nanocomposite.

Particulars of composition	Quantity of contribution to Al7075
Zinc (Zn)	05.560%
Copper (Cu)	01.620%
Aluminum (Al)	90.520%
Nickel (Ni)	00.030%
Titanium (Ti)	00.049%
Phosphorus (P)	00.0005%
Silicon (Si)	00.040%
Iron (Fe)	00.480%
Chromium (Cr)	00.183%
Magnesium (Mg)	01.520%
Others	Remaining

2.2. Selection of Process Parameters. Table 2 lists the criteria used in the selection process. The research was conducted to examine if process variables had a significant impact on kerf width during the WEDM process. Independent process variables include gap voltage and pulse times, like pulse-off and pulse-on, as well as discharge current; they were considered to minimize the kerf width. Such variables are obtained from machine manufacture catalogue and by trial runs. As they are sensitive to kerf width, they are confirmed. In machinability investigation on WEDM, one of the important responses is kerf width which is closely related to accuracy of machining in complicated profiles, so the response was kerf width (Kw) is preferred in this investigation to optimize the process parameters.

2.3. Experimental Setup and Experimentation. The ULTRACUT S1, Electronica made CNC type WEDM is employed for machining of SiC/Gr/Al7075 nanocomposite. The facility features are as follows: available table size is 370×600 mm, wire spool capacity is 6 kg, taper cutting angle is $\pm 5^{\circ}/100$ (max), auxiliary table traverse (u) is 30 mm, auxiliary table traverse (v) is also 30 mm, main table traverse X is 250 mm, and main table traverse Y is 350 mm. Needed power supply is AC 415 V $*$, 50 Hz, 3Φ. The work material is AL7075/SiC/graphite with the specimen size of $(100 \times 100 \times 8)$ mm. In machinability investigation on WEDM, one of the important responses is kerf width which is closely related to accuracy of machining in complicated profiles, so the response was kerf width (Kw) is preferred in this investigation to optimize the process parameters. The distilled water at 20°C was used as dielectric medium, and the 0.25 mm diameter sized uncoated brass wire and diffused and zinc coated brass wires (electrode) were used in this experimentation. Wire tension in oz is set as 4.

Figure 2: Synthesizing SiC/gr/Al7075 nanocomposite.

Table 2: Independent variables for WEDM.

Independent variables	Range of independent variables	
	Low	High
IP, discharge current	90	230
SV, gap set voltage	10	50
T_{off}, pulse-off time (μs)	40	60
T_{on}, pulse-on time (μs)	108	126

The Design-Expert software (v13) was employed for performing response surface methodology-based optimization. Among the available designs of response surface, the central composite full design was adapted as this investigation involved 4 variables. In case of unblocked category, the required number of runs is 31. The system generated variables levels for all 31 experiments (runs) provided in Table 3. The same was used to compare all three wire electrodes, namely, zinc coated, brass, diffused coated electrodes. The experimental work is shown in Figure 3(b), in which the measure of kerf width is gap distance.

2.4. Optimization by Response Surface Methodology. It is an assortment of numerical as well as factual approaches. It can be utilized for visualizing or analyzing influence of independent variables in desired response(s). The issues are the reaction of interest which is influenced by a few elements, with the purpose of expediting the reaction. The sort of link between the response and the free components is ambiguous in most RSM problems. The second-order model is with higher-degree polynomial to be considered for curvature features which is in the job profile. The approximating polynomials' parameters are estimated using the least squares approach. The fitted surface is then used to perform the response surface analysis. Four independent process variables such as gap voltage, pulse on times, discharge current, and pulse-off were considered to analyse their influence on kerf width while machining SiC/Gr/Al7075 nanocomposite.

The ranges of these independent process variables were established based on the pilot investigations. The levels of numerous measures, as well as their names, are shown in Table 2. The experimental observations were consolidated and are given in Table 3.

Table 3: Measured kerf width of brass, zinc coated, and diffused coated wires.

Run	T_{on}	T_{off}	IP	SV	Zinc coated	Brass	Diffused coated
1	117	50	160	30	0.303	0.318	0.315
2	126	50	160	10	0.295	0.335	0.332
3	117	60	160	10	0.289	0.335	0.332
4	117	60	230	30	0.301	0.334	0.331
5	117	50	160	30	0.307	0.332	0.329
6	126	40	160	30	0.317	0.333	0.330
7	126	50	160	50	0.329	0.339	0.336
8	126	60	160	30	0.306	0.321	0.318
9	117	50	160	30	0.304	0.319	0.316
10	108	50	90	30	0.318	0.334	0.331
11	117	50	230	50	0.311	0.333	0.330
12	117	40	160	10	0.317	0.326	0.322
13	117	50	160	30	0.304	0.330	0.327
14	117	50	90	50	0.313	0.329	0.326
15	108	50	160	50	0.298	0.313	0.310
16	117	50	160	30	0.311	0.313	0.310
17	117	40	160	50	0.303	0.318	0.315
18	117	40	230	30	0.309	0.335	0.332
19	108	50	160	10	0.318	0.334	0.331
20	117	50	160	30	0.305	0.320	0.317
21	117	50	90	10	0.318	0.334	0.331
22	108	50	230	30	0.297	0.312	0.309
23	117	50	160	30	0.305	0.334	0.331
24	117	60	160	50	0.318	0.334	0.331
25	108	40	160	30	0.303	0.335	0.332
26	126	50	90	30	0.31	0.326	0.322
27	126	50	230	30	0.316	0.332	0.329
28	108	60	160	30	0.3	0.315	0.312
29	117	50	230	10	0.301	0.327	0.323
30	117	60	90	30	0.305	0.334	0.331
31	117	40	90	30	0.318	0.339	0.330

3. Results and Discussion

3.1. Influence of Electrodes on Kerf Width Response. There were results of all 31 settings tested in this study. Zinc coated brass wire electrode offered less kerf width than the uncoated brass as well as diffused wire electrodes for machining Al/SiC

(a) (b)

Figure 3: (a) NPMD-WEDM experimental facility and (b) experimental work piece.

graphite hybrid composites. According to the literature, the kerf width is proportional to the melting temperature of the wire tool electrode material [20]. Because the exterior zinc coat has a low melting point compared to core brass wire electrode, the transmission of useful energy to work zone will be high as the rate of cooling of electrode increases. The prime cause for poor surface finish on work material is uneven thermal load of electrode (brass wire) leading to uneven generation of spark. The ineffective flushing is also a cause.

3.2. Influence of Independent Variables on Kerf Width. The experimental data given in Table 3 are analyzed using RSM with Design-Expert software which is described in the earlier section. Table 3 shows the kerf width results throughout 31 test runs. At the first glance, there are not much variations which identified that the result ranges from 297 to 323 μm for coated brass wire with zinc. Little more kerf width was obtained with use of uncoated brass wire from 312 to 335 μm. The performance of diffuse coated wire is superior to that of brass wire. The kerf width values for diffused wire range from 309 to 332 μm. The comparison of kerf width for brass, zinc coated, and diffused coated wires is presented in Figures 4 and 5, and in Figure 6, the average kerf width is shown. By using RSM, the proposed minimum kerf width (297 μm) can be achieved by the combination of T_{on} as 108, T_{off} as 50, IP of 230 A, and SV of 30 volts with zinc coated wire. From Figure 6, higher kerf width can be noticed when machining with raw brass wire and diffused coated wires. The average kerf width is achieved with zinc coated wire. The kerf width is found to increase as the T_{on} value rises. The cutting rate is increasing as the pulse-off time increases kerf width, with a large initial spike in cutting width value and subsequently a gradual decrease. In the second stage, the level is low. When it comes to peak current, we start by increasing it and then cut it off. In the second and third levels, the width value decreases.

3.3. Analysis of Variance (ANOVA). ANOVA was carried out at a 95% confidence level. In the analysis of variance, the F value performs the most important function for independent input variables. The ANOVA was used for exploring the impact of four independent input variables in WEDM of synthesized novel material in terms of kerf width. Table 4 show the ANOVA findings for Kw. The most dominant control factors on kerf width are pulse-off time (F value = 32.58), discharge current (F value = 31.23), and pulse-on time (F value = 21.51), according to the ANOVA table. Another key factor is the gap set voltage (SV) which secures F value of 16.35. The F value indicates the contribution of the factor to the response. The p value indicates the significance of contribution. If the p value is less than 0.05, the factor or such combination of factors is significantly influencing the response. That is, the response can be controlled by altering those factor levels. If the p value is greater than 0.1, this indicates that the factor or the combination of factors is not influencing the response. That is, the response could not be controlled by altering such parameters. From Table 4, it is understood that as all four factors considered yield p values less than 0.05, all factors considered in these investigations are significantly influencing the response of the kerf width; if more than 50% of the factors are significant, the statistical model is found to be good. In this case, 100% of the factors are significant; hence, the model is significant and statistically perfect. Except T_{off} vs IP, all factor combinations were also found to be significant. From Figure 4, it is evident that the zinc coated wire offered less kerf width than brass and diffused coated wires.

Figure 7 exhibits the RSM results about the accuracy of observations. More than 95% of observations are found to stick to the mean line, and only few observations are away from the mean line, called residual.

Figure 8 depicts the comparison of actual observations and predicted observations. The prediction could be obtained from (1). As these values are close to the central line, the mathematical model predictions are good and there is acceptable agreement with the experimental observations.

The construction of a normal probability plot of the residuals is a common check for the normality assumption. Under normalcy, each residual is shown against its expected value. Because this plot is a straight line (Figure 7), the residual distribution is found to be normal. The projected values and the actual values exhibit a linear graph, as shown in Figure 8. Figure 9 shows the deviation of kerf width with respect to experimental observations. This indicates the variation of kerf width response with respect to input parameters. That is, the input parameters could be optimized for

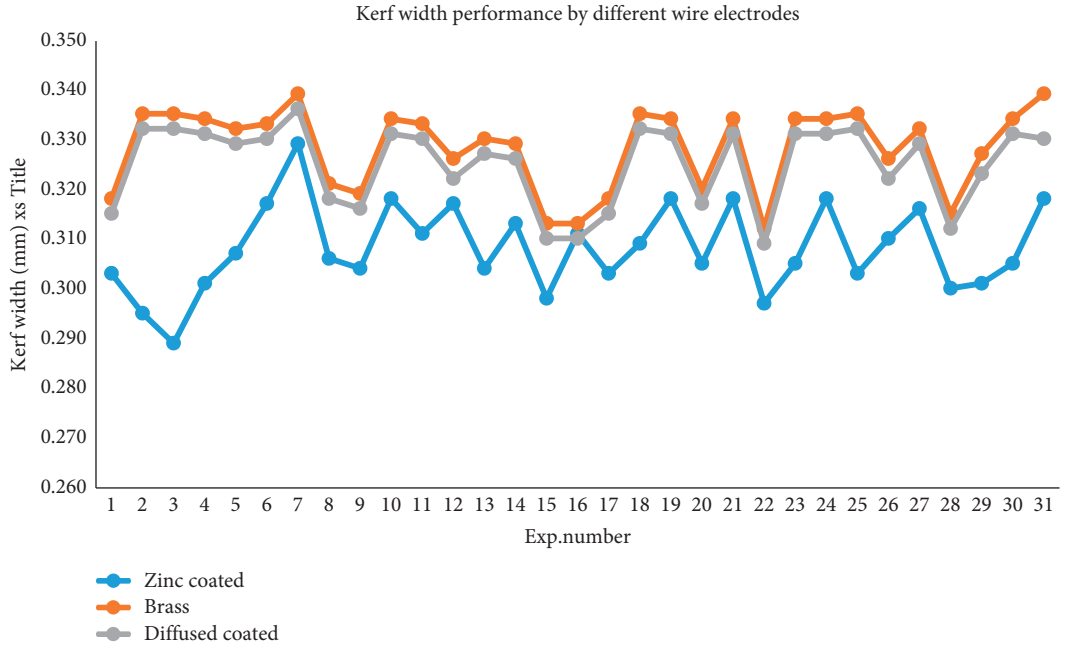

Figure 4: Comparison of kerf width performance by zinc coated, brass, and diffused wire electrodes.

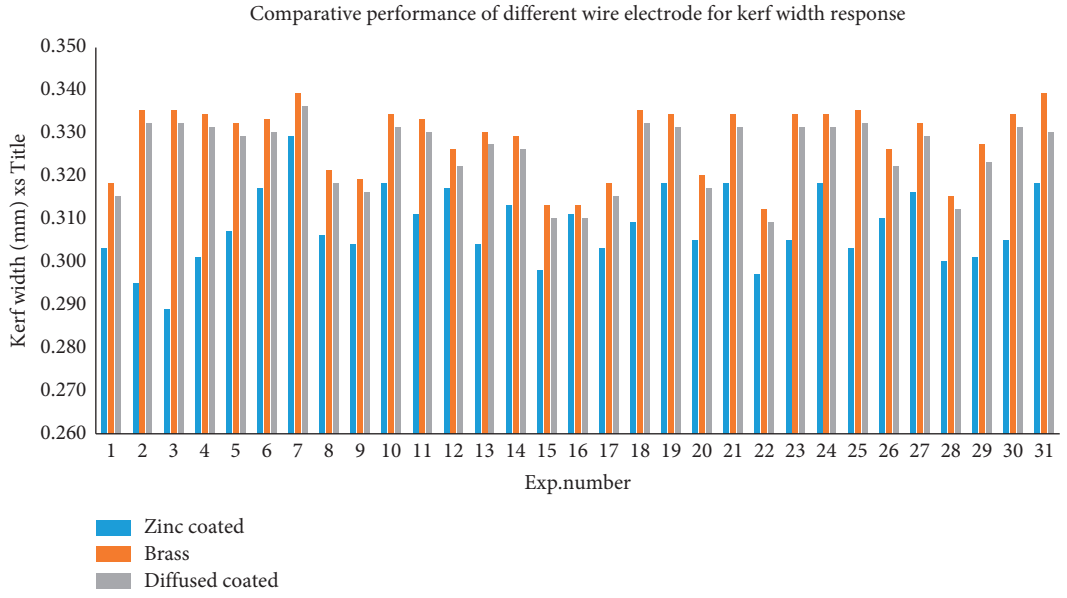

Figure 5: Comparison of kerf width for zinc coated, brass, and diffused wire electrodes.

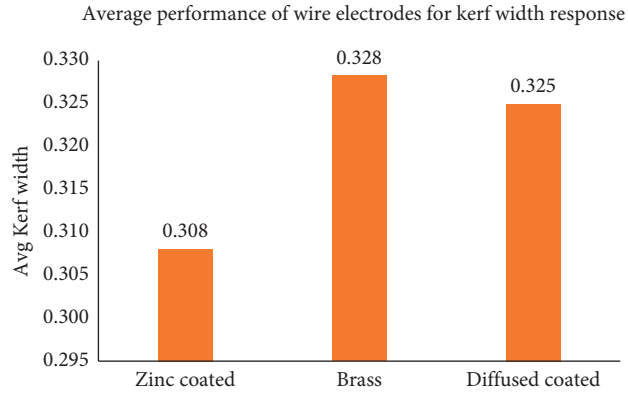

Figure 6: Average kerf width for zinc coated, brass, and diffused wire electrodes.

Table 4: ANOVA results for the response of kerf width.

Source	Sum of squares	Df	Mean square	F value	p value	
Model	0.0022	14	0.0002	26.33	<0.0001	Significant
A-T_{on}	0.0001	1	0.0001	21.51	0.0003	
B-T_{off}	0.0002	1	0.0002	32.58	<0.0001	
C-IP	0.0002	1	0.0002	31.23	<0.0001	
D-SV	0.0001	1	0.0001	16.35	0.0009	
T_{on} vs T_{off}	0.0000	1	0.0000	2.71	0.1189	
T_{on} vs IP	0.0002	1	0.0002	30.92	<0.0001	
T_{on} vs SV	0.0007	1	0.0007	123.69	<0.0001	
T_{off} vs IP	6.250E-06	1	6.250E-06	1.06	0.3184	
T_{off} vs SV	0.0005	1	0.0005	78.43	<0.0001	
IP vs SV	0.0001	1	0.0001	9.54	0.0070	
T_{on}^2	0.0000	1	0.0000	4.10	0.0598	
T_{off}^2	4.413E-06	1	4.413E-06	0.7488	0.3996	
IP^2	0.0001	1	0.0001	11.58	0.0036	
SV^2	0.0000	1	0.0000	5.95	0.0268	
Residual	0.0001	16	5.894E-06			
Lack of fit	0.0001	10	5.058E-06	0.6943	0.7095	Not significant
Pure error	0.0000	6	7.286E-06			
Correlation total	0.0023	30				

The F value helps to identify the contribution of particular process input in developing response of kerf width (Kw). The p value helps to identify the significance of a particular variable or combination of variables in the response of kerf width. If p value less than 0.05 for a particular variable or combination of variables, then it is considered sensitive in producing a response of kerf width. If a p value greater than or equal to 0.1 meant insignificant that is no sensitiveness in producing a response of kerf width.

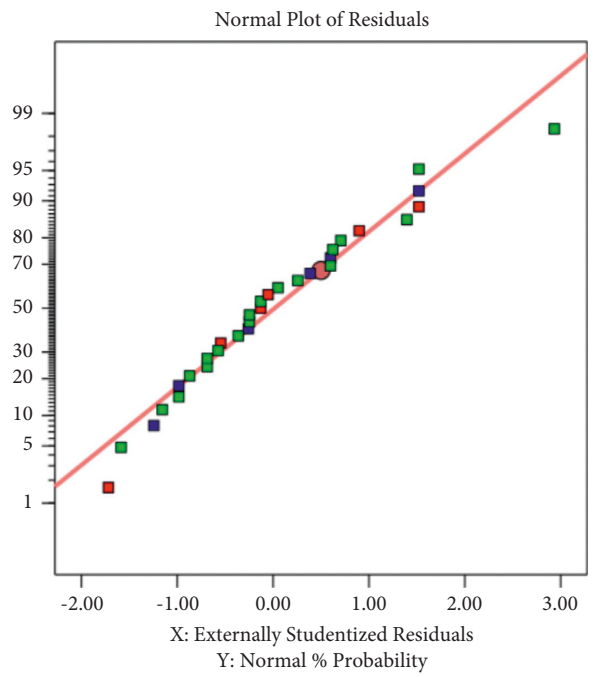

Figure 7: Accuracy of observations of kerf width.

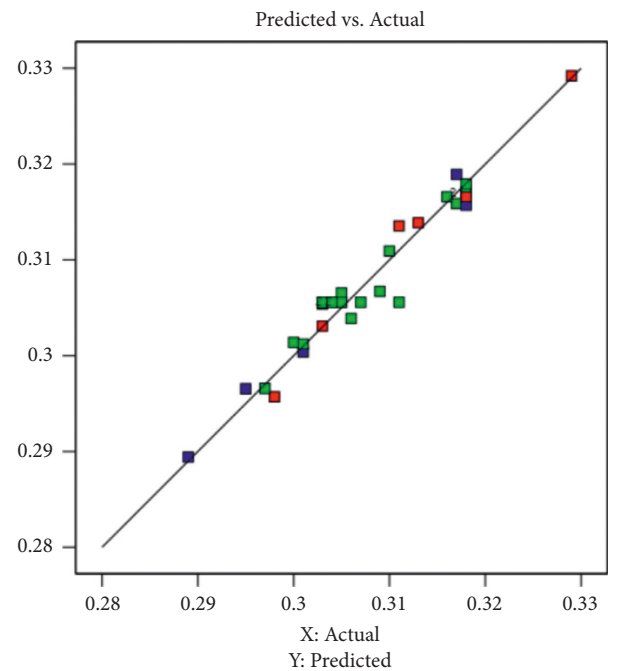

Figure 8: Predicted response versus actual response of kerf width.

the minimum kerf width. From Figure 9, it can be ensured that all observations are within the limits (red lines) and these observations did not statically violate assumption and can be acceptable. Hence, it is understood that the machinability of proposed composite is found to be good and controlling the kerf width is possible by varying the input parameters. Figure 10 shows the 3D surface plot which shows the interrelationship between the pulse-on time (T_{on}) and pulse-off time (T_{off}). Decrease of pulse-off time and pulse-on time decreases the kerf width to a certain extent, and more decrease was found at 108μs pulse-on time and 50μs pulse-off time.

Figure 11 is a 3D surface plot which depicts the relationship between the input current and pulse-on time influences on the kerf width variations. It indicates that increase of input current as well as decrease of pulse-on time decreases the kerf drastically. The optimal solutions are near input current of 230A and pulse-on time of 108μs. Figure 12 exhibits the relationship between the variation of gap voltage and pulse-on time on kerf

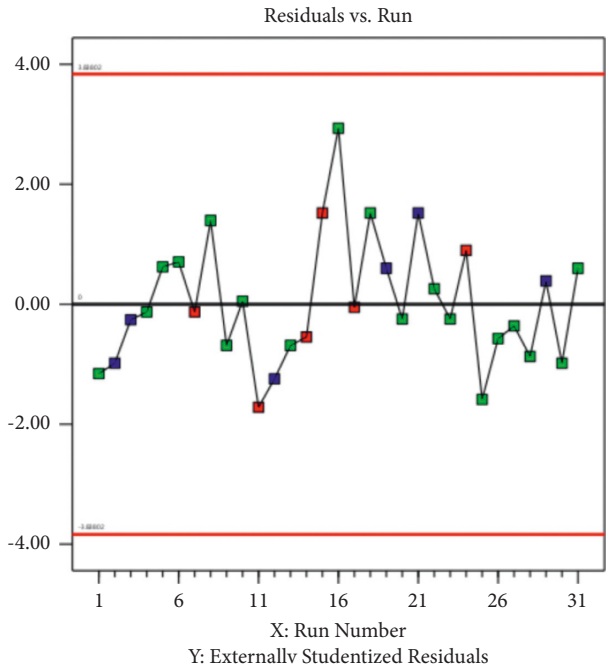

Figure 9: Residual on kerf width observations.

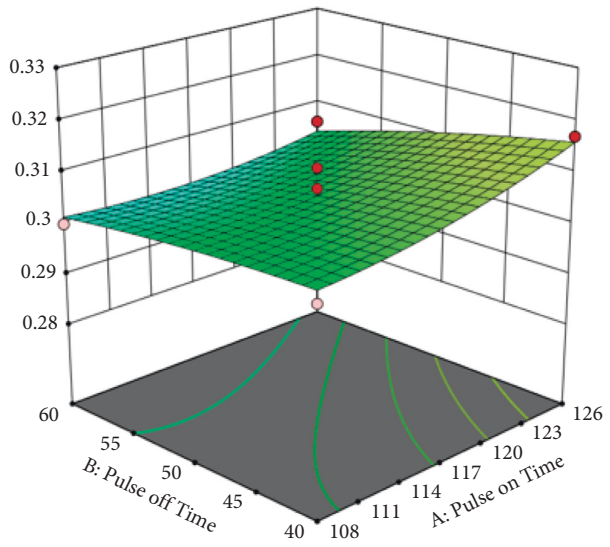

Figure 10: Joint performance on kerf width by T_{on} and T_{off}.

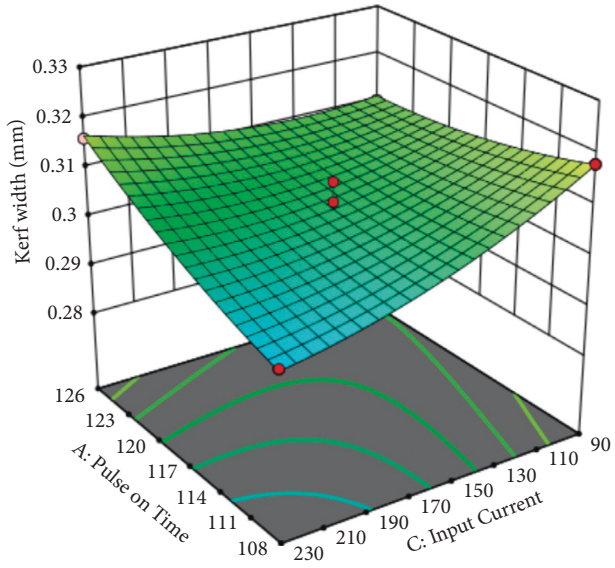

Figure 11: Joint performance on kerf width by T_{on} and IP.

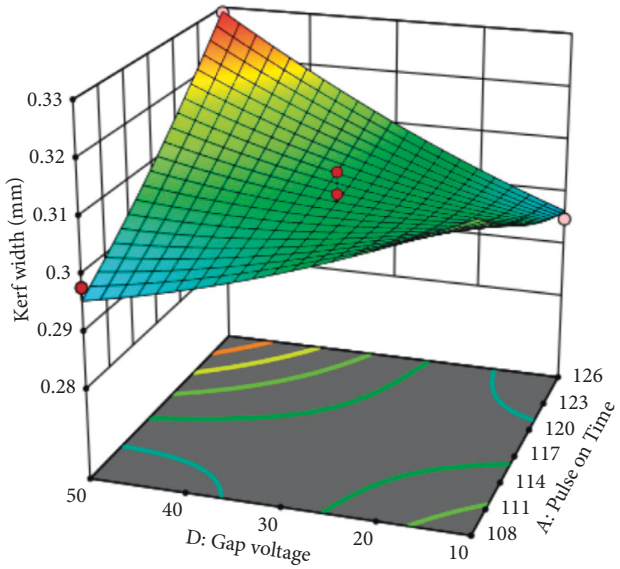

Figure 12: Joint performance on kerf width by T_{on} and SV.

width. Here, average gap voltage performs better. Figure 13 illustrates the relationship between the pulse-off time and input current. Increase of input current and decrease of pulse-off time decrease the kerf width. Figure 14 reveals the relationship between gap voltage and pulse-off time. Decrease of both helps to decrease the kerf width. Figure 15 explains the interrelationship between gap voltage and input current in the response of kerf width. The increase of input current and decrease of gap voltage help to decrease the kerf width. Hence, it is proven that the machinability performance recorded is very good, prediction model exhibits good agreement with experimental observations, and kerf width could be adjusted based on the accuracy of machining required for the job specific.

Experimental data was used to generate the mathematical model to predict the kerf width by means of four independent process variables, which is shown below. If the p value is greater than 0.01, those factors are insignificant as determined by ANOVA. The quadratic equation has been stripped of its components in (1). It is a mathematical model which is used to predict the response of kerf width for the combinations of inputs not experimented with. As the model is

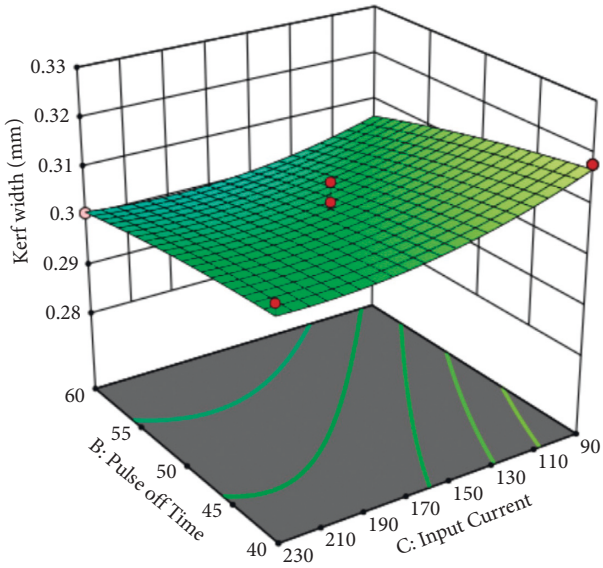

Figure 13: Joint performance on kerf width by T_{off} and IP.

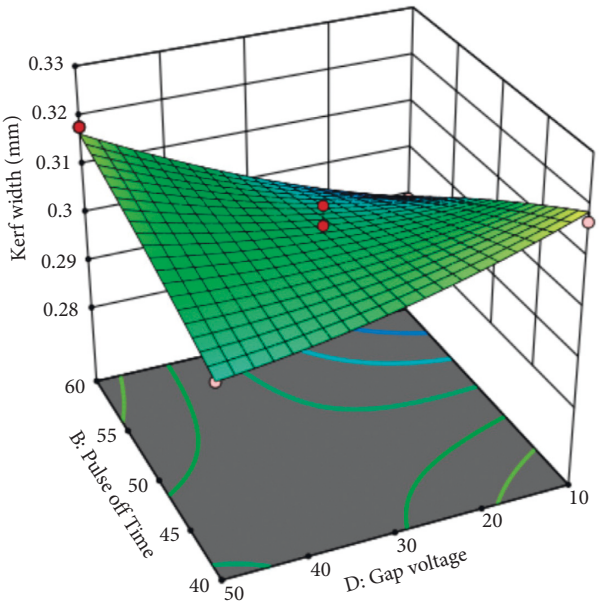

Figure 14: Joint performance on kerf width by T_{off} and SV.

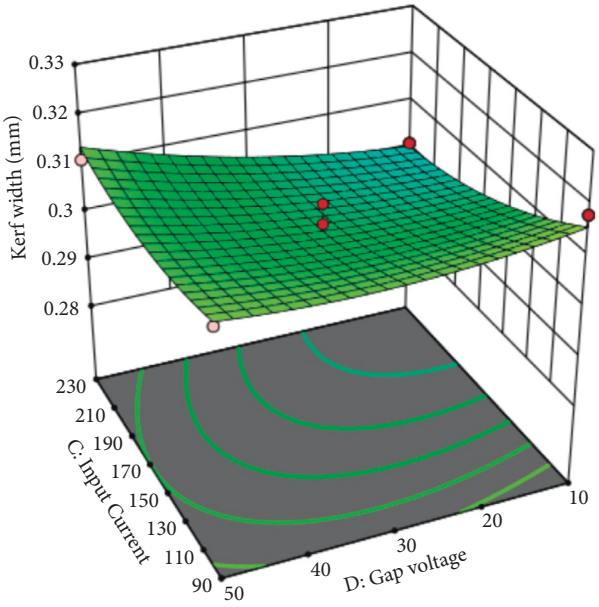

Figure 15: Joint performance on kerf width by IP and SV.

significant in the ANOVA table, the mathematical model has good agreement with the experimental results. Figures 10 to 15 depict the response surface of various combination factors on desired response (kerf width).

$$\begin{aligned}\text{Kerf width} = {} & 1.04193 - (0.00780556 * \text{TON}) + (0.0010875 * \text{TOFF}) - (0.00168092 * \text{IP}) - (0.0120815 * \text{SV}) \\ & - \left(2.22222^{e-05} * \text{TON} * \text{TOFF}\right) + \left(1.07143^{e-05} * \text{TON} * \text{IP}\right) + \left(7.5^{e-05} * \text{TON} * \text{SV}\right) + \left(1.78571^{e-06} * \text{TOFF} * \text{IP}\right) \\ & + \left(5.375^{e-05} * \text{TOFF} * \text{SV}\right) + \left(2.67857^{e-06} * \text{IP} * \text{SV}\right) + \left(2^{27072e-05} * \text{TON}^2\right) - \left(7.85714^{e-06} * \text{TOFF2}\right) \\ & + \left(6.30466^{e-07} * \text{IP2}\right) + 5.53571^{e-06} * \text{SV2}\big). \end{aligned} \tag{1}$$

The kerf width extended by the increase of T_{on} (Figure 10), it is seen that it increased with the increase in pulse-on time. One possible explanation is that as the extension of T_{on} increased the discharge energy, the output heat increased. Figure 11 shows that the increase of IP increased the kerf width due to the same reason behind the increase of T_{on} and, as a result, melting and evaporation rates. Figures 13 and 14 show that the gap set voltage is not influencing the kerf width significantly compared with other parameters.

4. Conclusion

The novel nanocomposite SiC/Gr/Al7075 was synthesized by stir casting method, and its machinability was investigated. As the composite was developed for special purpose of automotive and aerospace sectors and such components may have intricate shapes to machine, the machinability investigation carried out such feasible manufacturing process of wire EDM. The accuracy in machining sharp and intricate features depends on kerf width, so the response of kerf width was considered in the study. The response surface methodology-based experimental design and analysis were carried out. The set of experiments were repeated for three different wire electrodes, namely, uncoated brass wire and diffused and zinc coated brass wires. The performed set of readings was utilized for further process parameter optimization. The following are our findings.

(i) Machinability of the synthesized novel nanocomposite SiC/Gr/Al7075 by wire EDM process is ensured, and observations are statistically tested and found to be acceptable.

(ii) Among three different wire electrodes (uncoated brass wire and diffused and zinc coated brass wires), the zinc coated brass wire electrode outperformed the others in terms of minimal kerf width.

(iii) The minimal kerf width of 289 microns was recorded with use of zinc coated brass wire electrode under the process setting of 117 μs pulse-on time, 60 μs pulse-off time, 160A input current, and 10 volt gap voltage.

(iv) ANOVA results confirmed that all four process parameters are influencing significantly the machining quality and accuracy can be altered by altering the process inputs like pulse-on time, pulse-off time, input current, and gap voltage.

(v) The ranking of the influence of process parameters from high to low according to F value in the ANOVA results is as follows: pulse-off (F value = 32.58), discharge current (F value = 31.23), pulse-on time (F value = 21.51), and gap voltage (F value = 16.35).

Hence, the experimental investigation ensured the machinability of the synthesized novel nanocomposite SiC/Gr/Al7075 in WEDM process. Further investigation such as machinability investigation of micro milling process could be conducted.

Data Availability

The data used to support the findings of this study are included in the article. Should further data or information be required, these are available from the corresponding author upon request.

Conflicts of Interest

The authors declare that they have no conflicts of interest.

References

[1] F. Toptan, A. C. Alves, I. Kerti, E. Ariza, and L. A. Rocha, "Corrosion and tribocorrosion behaviour of Al–Si–Cu–Mg alloy and its composites reinforced with B_4C particles in 0.05 M NaCl solution," *Wear*, vol. 306, no. 1-2, pp. 27–35, 2013.

[2] H. Kala, K. K. S. Mer, and S. Kumar, "A review on mechanical and tribological behaviors of stir cast aluminum matrix composites," *Procedia materials science*, vol. 6, pp. 1951–1960, 2014.

[3] M. Imran and A. R. A. Khan, "Characterization of Al-7075 metal matrix composites: a review," *Journal of Materials Research and Technology*, vol. 8, no. 3, pp. 3347–3356, 2019.

[4] V. C. Uvaraja and N. Natarajan, "Optimization of friction and wear behaviour in hybrid metal matrix composites using Taguchi technique," *Journal of Minerals and Materials Characterization and Engineering*, vol. 11, no. 08, pp. 757–768, 2012.

[5] N. Radhika and R. Subramaniam, "Wear behaviour of aluminium/alumina/graphite hybrid metal matrix composites using Taguchi's techniques. Industrial lubrication and tribology," *Ndustrial Lubrication and Tribology*, vol. 63, 2013.

[6] S. K. Ravesh and T. K. Garg, "Preparation & analysis for some mechanical property of aluminium based metal matrix composite reinforced with SiC & fly ash," *International Journal of Engineering Research in Africa*, vol. 2, no. 6, pp. 727–731, 2012.

[7] B.-H. Yan and C.-C. Wang, "Machinability of SiC particle reinforced aluminum alloy composite material," *Journal of Japan Institute of Light Metals*, vol. 43, no. 4, pp. 187–192, 1993.

[8] J. Monaghan and P. O'reilly, "The drilling of an Al/SiC metal-matrix composite," *Journal of Materials Processing Technology*, vol. 33, no. 4, pp. 469–480, 1992.

[9] C.-C. Liu and J.-L. Huang, "Micro-electrode discharge machining of TiN/Si3 N4 composites," *British Ceramic Transactions*, vol. 99, no. 4, pp. 149–152, 2000.

[10] C.-C. Liu and J.-L. Huang, "Effect of the electrical discharge machining on strength and reliability of TiN/Si3N4 composites," *Ceramics International*, vol. 29, no. 6, pp. 679–687, 2003.

[11] L. Gao, J. Li, T. Kusunose, and K. Niihara, "Preparation and properties of TiN-Si3N4 composites," *Journal of the European Ceramic Society*, vol. 24, no. 2, pp. 381–386, 2004.

[12] C. Zhang, "Effect of wire electrical discharge machining (WEDM) parameters on surface integrity of nanocomposite ceramics," *Ceramics International*, vol. 40, no. 7, pp. 9657–9662, 2014.

[13] K. H. Ho, S. T. Newman, S. Rahimifard, and R. D. Allen, "State of the art in wire electrical discharge machining (WEDM)," *International Journal of Machine Tools and Manufacture*, vol. 44, no. 12-13, pp. 1247–1259, 2004.

[14] S. Vijaya Bhaskar, T. Rajmohan, G. R. Giri Sesha Sai, and G. Sandeep Kumar Reddy, "Multiple performance optimization in WEDM parameters using desirability analysis," in *Applied Mechanics and Materials,* vol. 813-814, pp. 352–356, Trans Tech Publications Ltd, 2015.

[15] T. Babu Rao and A. Gopala Krishna, "Simultaneous optimization of multiple performance characteristics in WEDM for machining ZC63/SiCp MMC," *Advances in Manufacturing*, vol. 1, no. 3, pp. 265–275, 2013.

[16] R. Bobbili, V. Madhu, and A. K. Gogia, "Effect of wire-EDM machining parameters on surface roughness and material removal rate of high strength armor steel," *Materials and Manufacturing Processes*, vol. 28, no. 4, pp. 364–368, 2013.

[17] K.-Y. Kung and K.-T. Chiang, "Modeling and analysis of machinability evaluation in the wire electrical discharge machining (WEDM) process of aluminum oxide-based ceramic," *Materials and Manufacturing Processes*, vol. 23, no. 3, pp. 241–250, 2008.

[18] A. Mandal, A. R. Dixit, A. K. Das, and N. Mandal, "Modeling and optimization of machining nimonic C-263 superalloy using multicut strategy in WEDM," *Materials and Manufacturing Processes*, vol. 31, no. 7, pp. 860–868, 2016.

[19] P.-H. Yu, H.-K. Lee, Y.-X. Lin, S.-J. Qin, B.-H. Yan, and F.-Y. Huang, "Machining characteristics of polycrystalline silicon by wire electrical discharge machining," *Materials and Manufacturing Processes*, vol. 26, no. 12, pp. 1443–1450, 2011.

[20] M. Azam, M. Jahanzaib, J. A. Abbasi, and A. Wasim, "Modeling of cutting speed (CS) for HSLA steel in wire electrical discharge machining (WEDM) using moly wire," *Journal of the Chinese Institute of Engineers*, vol. 39, no. 7, pp. 802–808, 2016.

[21] G. Anbuchezhiyan, B. Mohan, N. Senthilkumar, and R. Pugazhenthi, "Synthesis and characterization of silicon nitride reinforced Al–Mg–Zn alloy composites," *Metals and Materials International*, vol. 27, pp. 1–12, 2021.

[22] G. Anbuchezhiyan, T. Muthuramalingam, and B. Mohan, "Effect of process parameters on mechanical properties of hollow glass microsphere reinforced magnesium alloy syntactic foams under vacuum die casting," *Archives of Civil and Mechanical Engineering*, vol. 18, no. 4, pp. 1645–1650, 2018.

[23] J. Namanga, J. Foba, D. T. Ndinteh, D. M. Yufanyi, and R. W. M. Krause, "Synthesis and magnetic properties of a superparamagnetic nanocomposite "Pectin-Magnetite nanocomposite"," *Journal of Nanomaterials*, vol. 2013, Article ID 137275, 8 pages, 2013.

[24] M. R. Phate, S. B. Toney, and V. R. Phate, "Analysis of machining parameters in WEDM of Al/SiCp20 MMC using taguchi-based grey-fuzzy approach," *Modelling and Simulation in Engineering*, vol. 2019, Article ID 1483169, 13 pages, 2019.

[25] J. U. Prakash, P. Sivaprakasam, I. Garip et al., "Wire electrical discharge machining (WEDM) of hybrid composites (Al-Si12/B4C/fly ash)," *Journal of Nanomaterials*, vol. 2021, Article ID 2503673, 10 pages, 2021.

[26] I. V. Manoj, H. Soni, S. Narendranath, P. M. Mashinini, and F. Kara, "Examination of machining parameters and prediction of cutting velocity and surface roughness using RSM and ANN using WEDM of Altemp HX," *Advances in Materials Science and Engineering*, vol. 2022, Article ID 5192981, 9 pages, 2022.

[27] M. Taheri, M. Jahanfar, and K. Ogino, "Wear properties of nanocomposite traffic marking paint," *Journal of Nanomaterials*, vol. 2018, Article ID 2569249, 13 pages, 2018.

[28] S. Fernández de Ávila, J. C. Ferrer, J. L. Alonso, R. Mallavia, and B. Rakkaa, "Facile preparation of optically tailored hybrid nanocomposite," *Journal of Nanomaterials*, vol. 2014, Article ID 671670, 7 pages, 2014.

[29] Y. Zhu and J. Tao, "Thermally induced bistable functionally graded nanocomposite plate," *Mathematical Problems in Engineering*, vol. 2022, Article ID 1185792, 18 pages, 2022.

[30] P. Nguyen-Tri, T. A. Nguyen, P. Carriere, and C. Ngo Xuan, "Nanocomposite coatings: preparation, characterization, properties, and applications," *International Journal of Corrosion*, vol. 2018, Article ID 4749501, 19 pages, 2018.

[31] T. T. N. Anh, V. Van Thu, H.-S. Dang, V.-H. Pham, and P. D. Tam, "Cerium oxide/polypyrrole nanocomposite as the matrix for cholesterol biosensor," *Advances in Polymer Technology*, vol. 2021, Article ID 6627645, 10 pages, 2021.

[32] L. T. Tran, H. V. Tran, T. D. Le, G. L. Bach, and L. D. Tran, "Studying Ni(II) adsorption of magnetite/graphene oxide/chitosan nanocomposite," *Advances in Polymer Technology*, vol. 2019, Article ID 8124351, 9 pages, 2019.

[33] T. T. Nguyen, N. T. Pham, T. T. M. Dinh et al., "Electrodeposition of hydroxyapatite-multiwalled carbon nanotube nanocomposite on Ti6Al4V," *Advances in Polymer Technology*, vol. 2020, Article ID 8639687, 10 pages, 2020.

[34] S. Banerjee, W. Du, U. Sundar, and K. A. Cook-Chennault, "Piezoelectric and dielectric characterization of MWCNT-based nanocomposite flexible films," *Journal of Nanomaterials*, vol. 2018, Article ID 6939621, 15 pages, 2018.